phys. stat. sol. (a) **115**, 157 (1989)

Subject classification: 64.70; S8.15

Centro de Estudios en Semiconductores,
Departamento de Física, Facultad de Ciencias,
Universidad de Los Andes, Mérida (a)
and Ottawa-Carleton Institute for Physics, University of Ottawa[1]*) (b)*

$(CuIn)_x(AgIn)_yMn_{2z}Te_2$ Alloys

$T(z)$ Phase Diagram and Optical Energy Gap Values

By

M. QUINTERO (a), R. TOVAR (a), M. DHESI (b), and J. C. WOOLLEY (b)

Polycrystalline samples of $(CuIn)_x(AgIn)_yMn_{2z}Te_2$ alloys are used in lattice parameter, optical energy gap E_0, and differential thermal analysis (DTA) measurements and for various sections of constant x/y ratio, $T(z)$ diagrams are determined. The results indicate that for both the zinc-blende and chalcopyrite phases, ordering of the manganese occurs in the lower temperature range. In contradiction of previous data, it is shown that at temperatures of 200 °C and below, the ordered chalcopyrite α' is the equilibrium condition over the complete range of solid solubility in the adamantine structures. It is shown that the manganese ordering has negligible effect on the lattice parameter but that appreciable lattice parameter differences can occur with different annealing temperatures, these differences being attributed to changes in non-stoichiometry. However, the value of E_0 is appreciably affected by the manganese ordering and it is shown that E_0 gives a very convenient indication of the particular phase present in a single phase sample.

An polykristallinen $(CuIn)_x(AgIn)_yMn_{2z}Te_2$-Legierungsproben werden Messungen des Gitterparameters, der optischen Energielücke E_0 und der differentiellen Thermoanalyse (DTA) durchgeführt und für verschiedene Abschnitte mit konstantem x/y-Verhältnis werden $T(z)$-Diagramme bestimmt. Die Ergebnisse zeigen, daß sowohl für die Zinkblende- als auch die Chalkopyritphase im Niedertemperaturbereich Manganordnung auftritt. Im Gegensatz zu früheren Werten wird gezeigt, daß bei Temperaturen von 200 °C und darunter, das geordnete Chalkopyrit α' die Gleichgewichtsbedingung über den vollständigen Bereich der Löslichkeit in den Adamantine-Strukturen darstellt. Es wird gezeigt, daß Manganordnungseinfluß auf den Gitterparameter vernachlässigbar ist, daß jedoch beträchtliche Gitterparameterdifferenzen bei unterschiedlichen Temperungstemperaturen auftreten können; diese Differenzen werden Änderungen in der Nichtstöchiometrie zugeordnet. Der Wert von E_0 wird jedoch beträchtlich beeinflußt durch Manganordnung und es wird gezeigt, daß E_0 in bequemer Weise eine spezielle Phase in einer Einphasenprobe anzeigt.

1. Introduction

In recent work [1 to 3], semimagnetic semiconductor alloys (SMSA) based on the I–III–VI_2 compounds have been investigated. When the magnetic element concerned is manganese, in order to retain semiconductor behaviour, it is necessary to preserve the electron-to-atom ratio by replacing the pair (I–III) by two Mn atoms so that a series of alloys of the form $(I–III)_{1-z}Mn_{2z}VI_2$ have been produced and studied. In most cases, the range of solid solution in the adamantine structure is large, up to 0.72 in the case of $(AgIn)_{1-z}Mn_{2z}Te_2$ [2]. The composition range of these materials

[1]) Ottawa, Ontario K1N 6N5, Canada.

can be extended by including a II–VI compound or another I–III–VI_2 compound as a further component. Thus the alloy systems $Cd_{2x}(CuIn)_yMn_{2z}Te_2$, $Cd_{2x}(AgIn)_yMn_{2z}Te_2$, $Zn_{2x}(AgIn)_yMn_{2z}Te_z$, and $Zn_{2x}(CuIn)_yMn_{2z}Te_2$ ($x + y + z = 1$) have been investigated in some detail [1, 2, 4] with ranges of solid solution, lattice parameter, and optical energy gap values being determined. The $T(z)$ diagrams of $(CuIn)_{1-z}Mn_{2z}Te_2$ [5], $(AgIn)_{1-z}Mn_{2z}Te_2$ [5], and $(AgGa)_{1-z}Mn_{2z}Te_2$ [6] have been reported and also the $T(z)$ diagrams of various sections of the $Cd_{2x}(AgIn)_yMn_{2z}Te_2$ system [7]. The magnetic susceptibility behaviour has been studied for a number of such systems [6 to 10]. Here, the behaviour of the system $(CuIn)_x(AgIn)_yMn_{2z}Te_2$ ($x + y + z = 1$) has been studied.

In the case of SMSA based on the II–VI compounds, e.g. $Cd_{1-z}Mn_zTe_2$, the Mn atoms are distributed at random on the cation sublattice at all temperatures. However, in the case of the I–III–VI_2 derived alloys, various measurements have shown [3, 5, 10] that while the alloys can be produced with this random Mn configuration, the equilibrium condition at lower temperatures has the Mn atoms crystallographically ordered (or partially ordered) on the cation sublattice. This ordering has a pronounced effect on the optical energy gap values and on the magnetic properties so that the behaviour of the Mn-ordered and Mn-disordered alloys of the same composition are appreciably different [5, 10].

In order to investigate these differences, it is necessary to choose the heat treatment of single phase samples of the alloys so as to produce the required Mn-ordered or Mn-disordered conditions. For this purpose, a detailed knowledge of the T versus composition phase diagram is required. In the present work, measurements of DTA, lattice parameter, and optical energy gap values have been used to study the behaviour and $T(z)$ diagrams of various sections of the $(CuIn)_x(AgIn)_yMn_{2z}Te_2$ system.

2. Preparation of Alloys and Experimental Measurements

The compositions of the samples used in the measurements are shown in the composition diagram in Fig. 1. In order to produce useful $T(z)$ diagrams, samples were chosen to be on the sections given by $y = 0$, $x = 3y$, $x = y$, $3x = y$, and $x = 0$. Also, since the interest of the programme is in SMSA, in most cases the values of z were limited to the range $0 < z < 0.7$, and the MnTe-rich phases were not investigated.

All of the alloys used were produced by the usual melt and anneal technique [11]. The components of each 1 g sample were sealed under vacuum in a quartz capsule, which had previously been carbonized to prevent reaction of the alloys with the quartz. The components were then melted together at 1150 °C and homogenized by annealing at a lower temperature. In all such multicomponent systems, the appropriate temperature of anneal is not easily determined until the T versus composition diagrams is known. However, in the present case, the previous results for the sections $(CuIn)_{1-z}Mn_{2z}Te_2$ and $(AgIn)_{1-z}Mn_{2z}Te_2$ [5] showed that a temperature of 600 °C was satisfactory and this was used here. Initially, after this annealing, the samples were air-cooled to room temperature, and these samples were then used for the various measurements. However, it was found that the form of the T versus composition diagram was such that annealing at lower temperatures could produce alloys with different lattice parameters and energy gaps. This is discussed in more detail below.

The use of standard closed-tube differential thermal analysis (DTA) measurements, the determination of lattice parameter values using Debye-Scherrer and Guinier powder X-ray photographs, and the measurement of the room temperature optical energy gap by the standard transmission method have all been described in detail elsewhere [1, 12, 13].

3. Results and Discussion

The $T(z)$ diagrams obtained for the various sections are shown in Fig. 2, while the values of lattice parameter are given in Fig. 3 and 4 and the optical energy gap values are shown in Fig. 5. It is necessary to discuss these various sets of data together because of the effects each has on the others. Thus once phase boundaries have been determined from the DTA measurements, suitable annealing temperatures can be chosen for the samples used for the investigation of the variation of the values of lattice parameter, optical energy gap, etc. However, some near-vertical phase boundaries, e.g. limits of solid solubility and boundaries between the chalcopyrite α and zincblende β phases in the present diagram, are not easily detected from the DTA measurements. The lattice parameter and optical energy gap data must be used to provide the position of such boundaries. In addition, the optical energy gap data (and magnetic susceptibility data) have been found to give the best indication of the presence of ordering [5, 6]. In the present case, after the optical data had been obtained, the DTA curves had to be re-analyzed to give ordering temperatures previously not observed.

Turning to the individual results, Fig. 2a to e show the $T(z)$ diagrams for the sections $y = 0$, $x = 3y$, $x = y$, $3x = y$, and $x = 0$, respectively. In all of these sections, the data at $z = 0$ are consistent with the results previously shown in the $T(z)$ diagram of the $z = 0$ section [14]. The labelling of the various phase fields is consistent with that used previously for the initial $T(z)$ diagrams of the $y = 0$ and $x = 0$ section [5].

Thus α is the Mn-disordered chalcopyrite (dc), α' the Mn-ordered chalcopyrite (oc), β the Mn-disordered zincblende (dzb), and β' the Mn-ordered zincblende (ozb) phase. These are the phases of main interest in the present work. In addition, γ and δ are the NiAs and NaCl structures of MnTe, respectively, while β_2 is an In_2Te_3-rich phase in the Ag_2Te–In_2Te_3 section. Both δ and β_2 have compositions not represented by points in the present diagram. It is seen that there are wide ranges of solid solubility in all of the α, α', β, and β' phases. However, in the $T(z)$ diagrams previously presented for $(CuIn)_{1-z}Mn_{2z}Te_2$ ($y = 0$) and $(AgIn)_{1-z}Mn_{2z}Te_2$ ($x = 0$) sections [5], the limits of the α' phase were shown as $z = 0.35$ and $z = 0.40$, respectively. As indicated above,

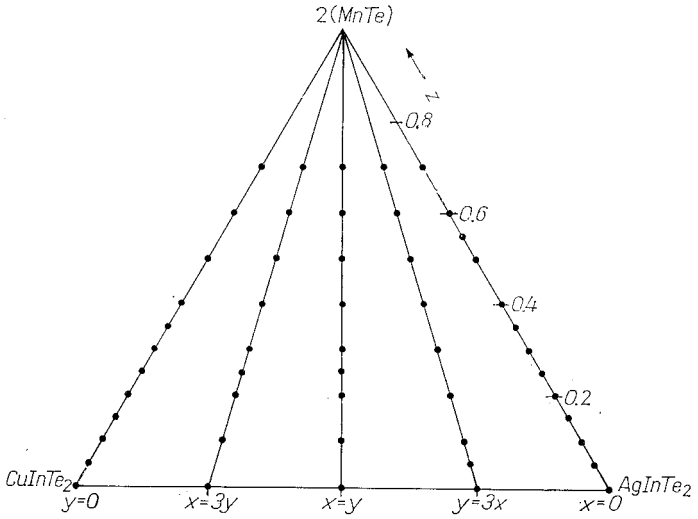

Fig. 1. Composition diagram for the $(CuIn)_x(AgIn)_yMn_{2z}Te_2$ alloy system investigated

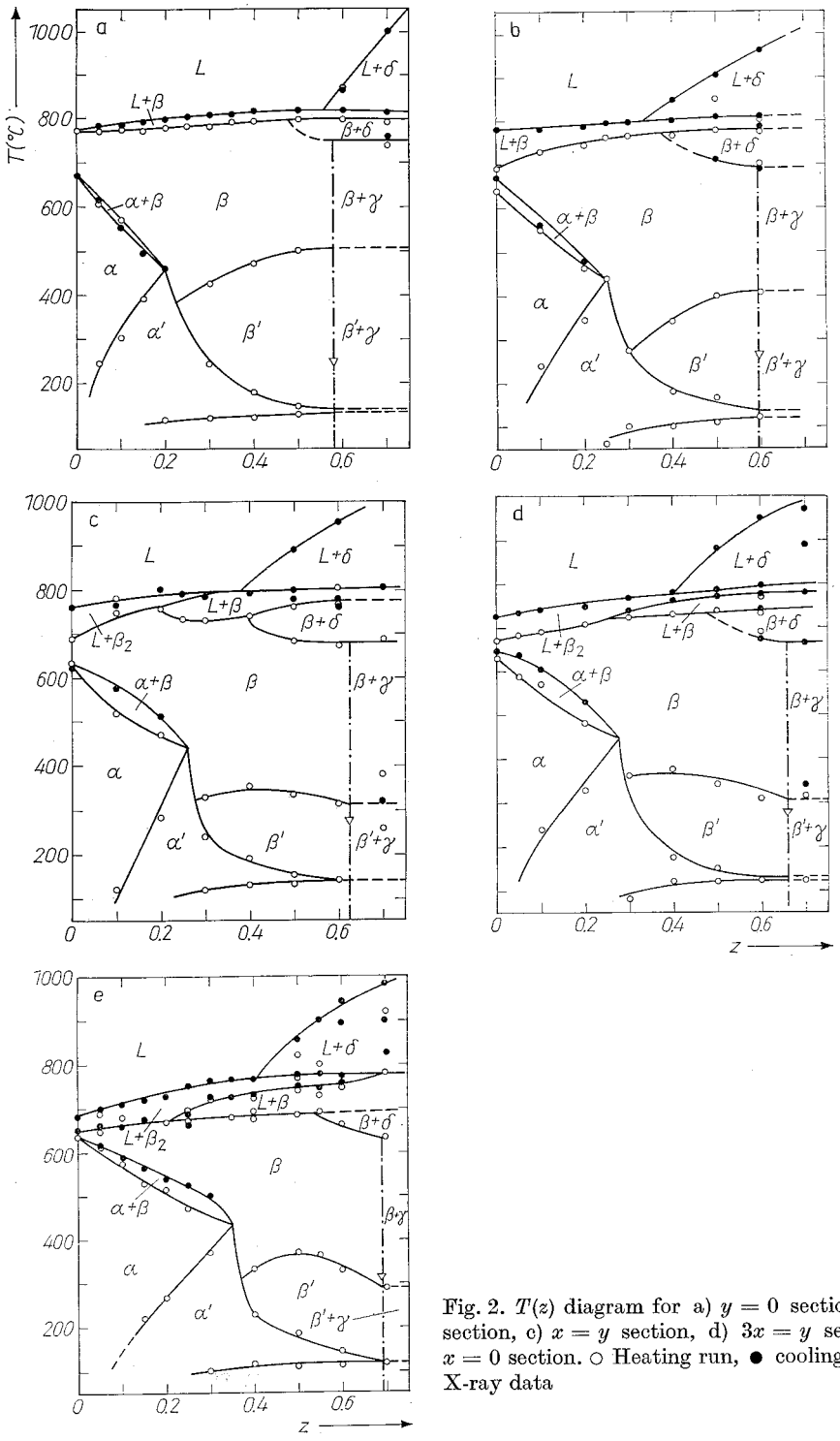

Fig. 2. $T(z)$ diagram for a) $y = 0$ section, b) $x = 3y$ section, c) $x = y$ section, d) $3x = y$ section, and e) $x = 0$ section. ○ Heating run, ● cooling run, ▽ from X-ray data

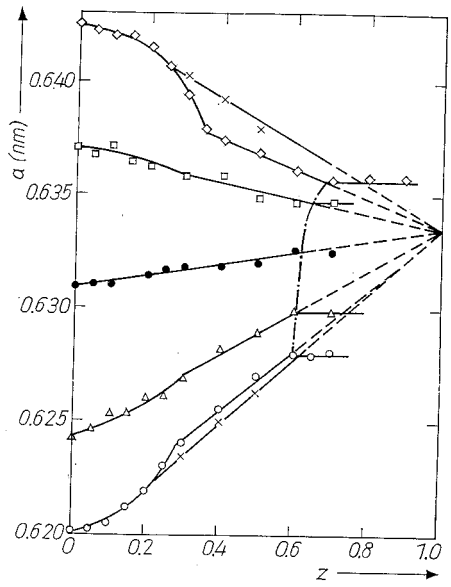

Fig. 3

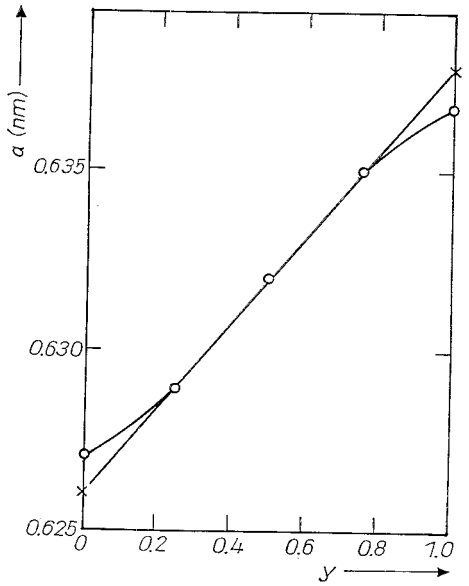

Fig. 4

Fig. 3. Variation of lattice parameter a with composition z. ○ $y = 0$, △ $x = 3y$, ● $x = y$, □ $y = 3x$, ◇ x = 0, x samples annealed at ≈ 100 °C for several weeks, —·— limit of solid solubility in adamantine phases

Fig. 4. Variation of lattice parameter a with composition y for alloys with $z = 0.5$; ○ samples air-cooled from 600 °C, x samples annealed at ≈ 100 °C

later measurements of magnetic susceptibility and optical energy gap showed that the α′ phase could be present in both cases to the limits of solid solubility in the adamantine phase [10]. Re-examination of the DTA data showed the presence at temperatures in the range 100 to 200 °C of small peaks corresponding to the α′–β′ transition. The modified α′–β′ phase boundaries are shown in Fig. 2a and f. For the other sections investigated here, the α′–β′ boundary showed the same form as is

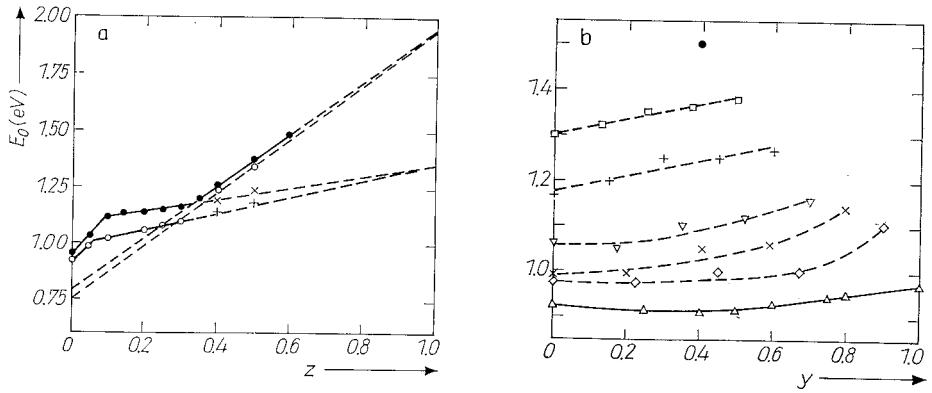

Fig. 5. Variation of energy gap E_0 with a) composition z; ● and × $x = 0$, ○ and + $x = y$, ● and ○ air-cooled from 600 °C, × and + annealed at ≈ 100 °C; b) composition y. △ $z = 0$, ◇ 0.1, × 0.2, ▽ 0.3, + 0.4, □ 0.5, ● 0.6

indicated in Fig. 2b to d, i.e. in all cases, the oc α' phase is the equilibrium condition at these lower temperatures. When these α'–β' transitions were being studied, in all cases a further transition was observed at temperatures of 120 °C or below, and the resulting lines are shown in Fig. 2. At the present time, there is no data to indicate the phase conditions below these boundaries.

Initially, X-ray powder photographs were taken of the samples which had been annealed at 600 °C and then air-cooled to room temperature. These photographs justified the field labelling of Fig. 2. In most cases, the alloys showed what appeared to be a zincblende phase and only for compositions close to $AgInTe_2$ the splitting of the lines due to $c/a < 2$ was observed. Close to $CuInTe_2$, no line splitting could be observed since $c/a = 2$ in this case, but faint chalcopyrite ordering lines were observed. For the $x = 0$ line, the value of c/a was found to increase from 1.966 at $AgInTe_2$ to a value of 2.0 at $z = 0.38$ while for the $z = 0$ line, c/a increased from the $AgInTe_2$ value to 2.0 at $y = 0.62$. The variation of a for these samples is shown in Fig. 3. It is seen for all except the $x = y$ line that at low z values the a versus z line is curved, this effect being largest for the $x = 0$ and $y = 0$ lines. At higher values of z, the a versus z lines show straight line form up to the limits of solid solubility in the adamantine phase. These limits can be seen in Fig. 3 as the points where the a versus z lines become horizontal, a showing a constant value in the two-phase range. In all of the cases shown the second phase was MnTe. In all cases, the linear parts of the a versus z curves are seen to extrapolate to the value of $a = 0.6335$ nm at $z = 1$, as has been found for a number of different systems [1, 2, 11, 15].

In previous work [1, 2], it was assumed that the change in the form of the a versus z line occurred at the composition at which the structure changed from chalcopyrite to zincblende. The present curves are consistent with this suggestion provided it is assumed that the samples represent conditions at ≈ 400 °C, which is not unreasonable for samples which were air-quenched from 600 °C. However, to investigate the lattice parameter values for the chalcopyrite phase in the composition range which is zincblende at 400 °C, samples with $z = 0.3$, 0.4, and 0.5 were annealed at $T \approx 100$ °C for several weeks. All of these samples gave X-ray photographs which appeared to be zincblende, i.e. no line splitting was observed, although from the $T(z)$ diagram and the optical energy gap data discussed below, the samples contained an appreciable amount of chalcopyrite phase. Thus it is seen that for the chalcopyrite phase at these higher z values $c/a = 2$, even in the case of the $(AgIn)_{1-z}Mn_{2z}Te_2$ section. The values of the lattice parameter a were determined for these samples, but only in the case of the lines $x = 0$ and $y = 0$ the difference between these values and those for the air-quenched samples was significantly different from the experimental scatter. The values for the lines $x = 0$ and $y = 0$ are shown in Fig. 3. It is seen that using these low temperature values, the variation of a with z is much closer to a straight line with linear behaviour for $z > 0.15$ and with curvature only for $z < 0.15$. It is of interest to note that these lines still extrapolate to the value of $a = 0.6335$ at $z = 1$. Previously [1, 2] it had been suggested that the curvature in the a versus z lines was due to non-stoichiometry in the chalcopyrite phase. While this explanation probably still applies to the curvature in the range $0 < z < 0.15$, the question now arises as to whether the effects observed in the water-quenched samples at higher values of z are related to the change with increasing z from chalcopyrite to zincblende structure. However, if this were the case, there should be no difference in lattice parameter between the air-cooled and low-temperature annealed samples for the cases of $z = 0.3$ and 0.35 where both treatments produce chalcopyrite conditions. Thus it appears probable that the differences in lattice parameter observed for a given composition are still due to differences in non-stoichiometry and that these in turn are related to the

temperatures at which the samples were equilibrated. With this in mind, it is of interest to see the variation of a with y for the $z = 0.5$ samples shown in Fig. 4. For the samples annealed at low temperatures, the variation of a with y is linear within the limits of experimental error, indicating the same degree of non-stoichiometry for all samples. However, for the air-quenched samples the a versus z line shows appreciable deviation from linearity, these deviations being of opposite sign for the AgIn and CuIn ends of the line. This appears to be related to the different directions of curvature of the a versus z lines close to $z = 0$ for the $x = 0$ and $y = 0$ lines. This dependence of the degree of non-stoichiometry on the temperature of equilibration could explain the range of values of the lattice parameter listed in the literature for $AgInTe_2$ [16].

With regard to the optical energy gap values, again the majority of the values were taken for the air-cooled samples and these are shown in Fig. 5. It is seen that E_0 varies mainly with z, showing little variation with the x/y ratio. Thus to present clearly all of the measured E_0 values, these are shown in Fig. 5 b plotted as a function of y for various constant values of z. However, in order to discuss the extrapolation to $z = 1$, the variation of E_0 with z is shown in Fig. 5 a for the cases of $x = 0$ and $x = y$. It is seen that these E_0 versus z graphs fall clearly into three sections. There is a small range with $z < 0.1$ corresponding to the alloys with dc structure α [5]. As has been indicated in previous cases [4, 6], these lines extrapolate to a value in the range 2.2 to 2.8 eV at $z = 1$, a value which characterizes the dc structure. However, the range of z is too small for any accurate estimate of this aiming point to be made. In the range $0.1 < z < 0.3$, the E_0 values clearly extrapolate to an aiming point at $z = 1$ of 1.35 eV, which is the value characteristic of the oc structure. Above $z = 0.3$, the points lie on a different line which has an aiming point of 1.95 eV, characteristic of the ozb structure [1, 2, 4]. Thus the air-cooled samples with $z = 0.4$ and 0.5 showed an E_0 value typical of the ozb structure. Absorption measurements were then made on the samples with $z = 0.4$ and 0.5, which had been annealed at $\approx$100 °C. For these samples, two absorption edges were observed. The lower energy values, as shown plotted in Fig. 5 a, fit well to the line corresponding to the oc phase, consistent with the $T(z)$ data. The higher E_0 values were found to be those of the ozb phase, indicating that at this low temperature the annealing times had not been long enough to allow the equilibrium conditions to be attained throughout the complete sample.

One further extrapolation which can be usefully carried out on the data in Fig. 5 a is the extrapolation of the E_0 values in the ozb range to $z = 0$. For the five different x/y ratios investigated here, these extrapolated values lay in the range 0.7 to 0.85 eV. These represent the E_0 values for the compounds $CuInTe_2$ and $AgInTe_2$ and the intermediate alloys in the cubic zincblende form, and the present data are in good agreement with values obtained previously for these results indicating that, for this set of compounds, the difference between the measured E_0 for the chalcopyrite form and the extrapolated E_0 for the zincblende form is of the order 0.25 eV in each case. Various theoretical studies have been made to estimate the value of this difference (ΔE_0) for the different chalcopyrite compounds. Thus Zunger [17] indicates that $\Delta E_0 = 0.4$ eV for most of these compounds, while Rincon [18] predicts values lying in the range 0.42 to 0.50 eV for the compounds considered here. It is seen that the values estimated by the present extrapolation method are appreciably smaller than these theoretically proposed values.

4. Conclusions

The DTA results indicate that the lines $x = 3y$, $x = y$, and $3x = y$ show very similar $T(z)$ diagrams to the $x = 0$ and $y = 0$ lines previously investigated [5]. However, for all sections it is found, as previously indicated by measurements of magnetic suscep-

tibility, that at low temperatures (below 200 °C) the α' chalcopyrite phase extends to the limits of solid solubility in the adamantine structure. It is then found, particularly for the limiting sections $x = 0$ and $y = 0$, that the variation of lattice parameter a with z is much closer to the linear form if measurements are made on samples annealed in the temperature range of the chalcopyrite phase. Because the c/a ratio has the value 2 for $z < 0.35$, the difference between chalcopyrite and zincblende structures is not easily observed in the X-ray photographs, but the measurements of optical energy gap clearly indicate the presence of the chalcopyrite phase in the samples annealed at low temperatures.

Extrapolation of the E_0 values to $z = 0$ in the zincblende range gives values of the order 0.25 eV for the difference between the measured energy gaps of the chalcopyrite materials and the extrapolated values corresponding to the same materials with zincblende form. These values are appreciably smaller than the theoretically predicted ones [17, 18].

Acknowledgements

The authors wish to thank Mr. G. S. Pérez and Mr. F. Sanchez for technical assistance. They are grateful to Consejo de Desarrollo Cientifico, Humanistico y Tecnologico (CDCHT) and Consejo Nacional de Investigationes Cientificas y Tecnologicas (CONICIT), Venezuela, for financial support.

References

[1] M. QUINTERO, L. DIERKER, and J. C. WOOLLEY, J. Solid State Chem. **63**, 110 (1986).
[2] M. QUINTERO and J. C. WOOLLEY, phys. stat. sol. (a) **92**, 449 (1985).
[3] A. ARESTI, L. GARBATO, A. GEDDO-LEHMANN, and P. MANCA, Proc. 7th Internat. Conf. Ternary and Multinary Compounds, Materials Research Society, Pittsburgh (PA) 1987 (p. 497).
[4] C. NEAL, J. C. WOOLLEY, R. TOVAR, and M. QUINTERO, J. Phys. D, in the press.
[5] M. QUINTERO, P. GRIMA, R. TOVAR, G. S. PÉREZ, and J. C. WOOLLEY, phys. stat. sol. (a) **107**, 205 (1988).
[6] M. QUINTERO, R. TOVAR, M. AL-NAJJAR, G. LAMARCHE, and J. C. WOOLLEY, J. Solid State Chem. **75**, 136 (1988).
[7] M. QUINTERO, E. GUERRERO, P. GRIMA, and J. C. WOOLLEY, J. Electrochem. Soc. **136**, 1220 (1989).
[8] M. QUINTERO, P. GRIMA, R. TOVAR, R. GOUDREAULT, D. BISSONNETTE, G. LAMARCHE, and J. C. WOOLLEY, J. Solid State Chem. **76**, 210 (1988).
[9] M. QUINTERO, P. GRIMA, J. E. AVON, G. LAMARCHE, and J. C. WOOLLEY, phys. stat. sol. (a) **108**, 599 (1988).
[10] G. LAMARCHE, J. C. WOOLLEY, R. TOVAR, M. QUINTERO, and V. SAGREDO, J. Magnetism magnetic Mater., in the press.
[11] R. BRUN DEL RE, T. DONOFRIO, J. E. AVON, J. MAJID, and J. C. WOOLLEY, Nuovo Cimento D **2**, 1911 (1983).
[12] R. G. GOODCHILD, O. H. HUGHES, S. A. LOPEZ-RIVERA, and J. C. WOOLLEY, Canad. J. Phys. **60**, 1096 (1982).
[13] M. QUINTERO, P. GRIMA, E. GUERRERO, R. TOVAR, and J. C. WOOLLEY, J. Crystal Growth **89**, 301 (1988).
[14] E. GUERRERO, M. QUINTERO, and J. C. WOOLLEY, J. appl. Phys. **63**, 2252 (1988).
[15] S. MANHAS, K. C. KHULBE, D. J. S. BECKETT, G. LAMARCHE, and J. C. WOOLLEY, phys. stat. sol. (b) **143**, 267 (1987).
[16] J. L. SHAY and J. H. WERNICK, Ternary Chalcopyrite Semiconductors: Growth, Electronic Properties and Applications, Pergamon Press, New York 1975 (p. 4).
[17] A. ZUNGER, Appl. Phys. Letters **50**, 164 (1987).
[18] C. RINCON, Solid State Commun. **64**, 663 (1987).

(Received May 22, 1989)